

Thermalization in different phases of charged SYK model

Tousik Samui^a and Nilakash Sorokhaibam^b

^a*Harish-Chandra Research Institute, Homi Bhabha National Institute
Chhatnag Road, Jhansi, Allahabad 211019, India*

^b*National Institute of Science Education and Research, HBNI, Bhubaneswar 752050, Odisha,
India*

E-mail: tousiksamui@hri.res.in, nilakash@niser.ac.in

ABSTRACT: We study thermalization of charged SYK model in two different phases. We show that both the chaotic phase and the integrable phase thermalize. Surprisingly the integrable state thermalizes instantaneously. While the chaotic state thermalizes exponentially fast. We also show that the introduction of random mass deformation ($q=2$ SYK term) slows down thermalization but the system thermalizes exponentially fast. This is observed despite the fact that large ($q=2$) SYK interaction forces spectral statistics to obey Poisson statistics. An interesting new observation is that the effective temperature is non-monotonic during thermalization in the chaotic state. It has a bump at relatively long time before settling down to the final value. With non-zero chemical potential, the effective temperature oscillates noticeably before settling down to the final value. We also find that the spectral asymmetry frequency does not change during quantum quenches.

Contents

1	Introduction and Summary	1
2	SYK model with complex fermions	7
2.1	Kadanoff-Baym equations and quantum quenches	9
3	Charged SYK model	12
3.1	Thermalization in the chaotic state	13
3.2	Thermalization in the integrable state	15
4	$(q = 2, 4)$ SYK model	19
5	Conclusions	20
	Bibliography	21

1 Introduction and Summary

Non-equilibrium dynamics of interacting quantum systems has been a subject of great interest for a long time [1, 2]. It is a subject of interest in various fields of physics, e.g. various aspects of condensed matter physics, heavy ion collisions, AdS/CFT and black hole dynamics, quantum cosmology, etc. It also has wide applications in engineering sciences (e.g. working principle of everyday semiconductor devices), biophysics (e.g. application in protein folding), etc. It is also the underlying principle for the impending rise of quantum computers in the next few decades [3].

In this paper we will examine non-equilibrium dynamics of chaotic quantum systems. We will be considering closed quantum systems. It is generally expected that these systems thermalize. We will be considering thermalization in the sense that, starting from an equilibrium state, after some finite perturbation the system comes back to equilibrium.¹ The most interesting aspect of this work is that we find certain special states which thermalize instantaneously.

¹We will not be considering thermalization of pure excited states.

Our interest is focused on Sachdev-Ye-Kitaev (SYK) models [4–6]. These are chaotic quantum systems consisting of N fermions with all-to-all random interactions.² It has recently been proposed that these models have special states which do not thermalize [7]. Surprisingly, we find that these states thermalize instantaneously. Non-equilibrium dynamics of SYK models and other related models has been studied in [8–12]. Pure excited states of SYK models has been studied in [13–15].

First we will briefly clarify on what we meant by a chaotic quantum system. There are various diagnostics of quantum chaos. The two most popular and well studied diagnostics are comparison of spectral statistics with random matrix theory (BGS conjecture, [16]) and exponential decay of Out-of-Time-Ordered correlators (OTOC) [17]. For a system like SYK model with widely separate time scales of dissipation and scrambling, OTOC decays exponentially. Considering the operators to be the microscopic fermionic degrees of freedom, the OTOC is

$$\begin{aligned} C(t) &= \text{Tr} \langle e^{-\beta H_{SYK}/4} \Psi_i^\dagger(t) e^{-\beta H_{SYK}/4} \Psi_j^\dagger(0) e^{-\beta H_{SYK}/4} \Psi_i(t) e^{-\beta H_{SYK}/4} \Psi_j(0) \rangle \\ &= f_0 - \frac{f_1}{N} e^{\lambda t} + \mathcal{O}(N^{-2}) \end{aligned} \quad (1.1)$$

where H_{SYK} is the Hamiltonian. We have taken the regularized OTOC as in [17].

We will mostly be working with two-fermion ($q = 2$), four-fermion ($q = 4$) and six-fermion ($q = 6$) all-to-all random interactions. So the Hamiltonian is

$$\begin{aligned} H_{SYK}(t) &= \mu \sum_i \Psi_i^\dagger \Psi_i + \sum_{i,j=1}^N j_{2,ij}(t) \Psi_i^\dagger \Psi_j + \sum_{i,j,k,l=1}^N j_{4,ij;kl}(t) \Psi_i^\dagger \Psi_j^\dagger \Psi_k \Psi_l \\ &\quad + \sum_{i,j,k,l,m,n=1}^N j_{6,ijk;lmn}(t) \Psi_i^\dagger \Psi_j^\dagger \Psi_k^\dagger \Psi_l \Psi_m \Psi_n \end{aligned} \quad (1.2)$$

Since we will be performing quantum quenches, we have considered time-dependent interactions except for the mass term. The mass term introduces an effective chemical potential $\eta = \mu$. Besides this, the mass term does not give rise to any new interesting physics. Quantum quenches using time-dependent mass is trivial in 0+1D systems [7]. As soon as the time dependence of the mass term stops, the system reach the final thermal equilibrium which has the same temperature as the initial state but with a different chemical potential. So in some sense, the system thermalizes instantaneously when quantum quench is performed using time dependent mass term (mass quench). We can also consider explicitly turning on chemical potential η in which case the total effective chemical potential is $\eta + \mu$.

²The original SYK model consists of Majorana fermions but we will be considering complex fermions with which the model has a conserved charge other than the Hamiltonian.

It has been shown that in the presence of chemical potential there is a first order phase transition [7, 18, 19]. The phase transition is between the chaotic phase and the integrable phase. The phase diagram is produced in [19]. The phase transition happens in a finite range of the chemical potential η . There is also a range of temperature in which the system can be in either of the two phases. In the chaotic phase, the system is strongly interacting and there is no quasi-particle dynamics. While in the integrable phase, the system consists of weakly interacting quasi-particles. This is evident from the plot of the spectral function in the integrable phase. For the sake of simplicity the phase transition is always studied without the two-fermion random interaction ($q = 2$) term.

The Lyapunov exponent of the chaotic phase is suppressed exponentially when the chemical potential is turned on [7, 20]. This implies that chaos is suppressed. The Lyapunov exponent in the integrable phase has also been calculated in [7]. Figure 1 is a reprint of the plot of the normalized Lyapunov exponent for the two different phases with varying temperature and a fixed chemical potential. It is effectively zero at very low temperature. But surprisingly it is non-zero and large at relatively high temperature especially in the temperature range where the system can exist in either of the two phases.

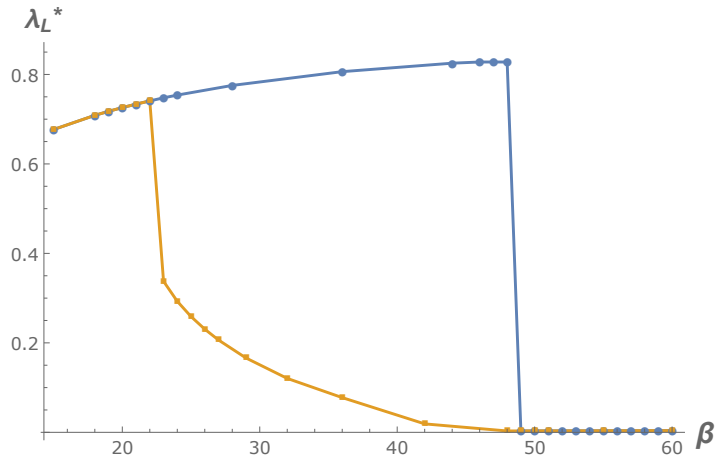


Figure 1: Normalized Lyapunov exponent with varying inverse temperature in the two different phases for $\eta = 0.27$ (reprinted from [7]). The sharp changes in the blue (orange) curve represents the transition from the chaotic (integrable) state to the integrable (chaotic) state. So, the blue (orange) curve mostly constitutes the chaotic (integrable) phase.

It is conventional wisdom that quantum chaos implies thermalization. So this suggests that turning on the chemical potential will slow down the thermalization pro-

cess in the chaotic phase. We will indeed find this to be the case. With the same reasoning, we expect that the integrable state would not thermalize at very low temperature. At higher temperature in the integrable phase, we still expect that the system would not thermalize because the system is still described by a very weakly interacting theory. Surprisingly, we will find that the system in the integrable state thermalizes instantaneously. The final state is a thermal state with a different temperature and a different chemical potential as compared to the initial state. This is somewhat similar to the instantaneous thermalization of mass quench. So, we expect that the instantaneous thermalization of the integrable state has an underlying physics different from the chaotic dynamics. Highly chaotic systems thermalize exponentially fast [8]. We also like to point out that in purely ($q=2$) SYK model, the system also equilibrates instantaneously but the final state is not a thermal state [9].

The ($q = 2$) SYK term is an integrable interaction. The $j_{2,ij}$ couplings can be diagonalized resulting in a theory of free N fermions with random masses. There is no sharp phase transition if we consider the ($q = 2, 4$) SYK model and put the chemical potential to zero [7]. The Lyapunov exponent is suppressed by the integrable interaction. We calculate the Lyapunov exponent of this system to high precision. But it does not sharply go to zero even when the ($q = 2$) interaction strength is very strong and at very low temperatures. This implies that this system is always in the chaotic phase. The system should thermalize exponentially fast. We will numerically show that this is true.

We show that the chaotic states thermalize exponentially fast by calculating the effective temperature during the non-equilibrium dynamics. Without chemical potential, the effective temperature has a single bump before settling down to the final value. With non-zero chemical potential, besides the bump the effective temperature oscillates noticeably before settling down to the final value. The oscillation frequency depends on the chemical potential and the momentum cutoff used to calculate the temperature.

Spectral asymmetry frequency (SAF) is the shift in the peak of the product of the retarded Green's function and advanced Green's function [21]

$$G^R(\omega)G^A(\omega) = \Phi(\omega - \omega_s) \quad (1.3)$$

$\Phi(\omega)$ is an even function of ω . ω_s is also the position of the peak of the spectral function $A(\omega) = -2\text{Im}G^R(\omega)$. This is an interesting quantity which remains unchanged when we perform quantum quenches using time dependent SYK terms. Other quantities like chemical potential and temperature changed when we compare the final state and the initial state after such a quantum quench. More details can be found in section 3.1.

For a chaotic system the spectral statistics is described by Wigner-Dyson (WD) statistics. For a generic integrable system, the spectral statistics is described by Poisson

distribution. It has been shown that ($q = 2$) SYK interaction forces the spectral statistics towards Poisson distribution [22].³ This exercise was done considering finite size systems and numerically diagonalizing the Hamiltonian. But as we have mentioned above, the system is always chaotic and always thermalize. So, this is a shortcoming of the BGS conjecture. It is hard to quantify how chaotic a system is or if the system is completely integrable. There has been other works in similar line where the spectral statistics is not WD statistics but the system is nevertheless highly chaotic [24].

The technical results of this work are:

1. We show that both the chaotic state and the integrable state in charged SYK model thermalize. A system in the integrable state thermalizes instantaneously.
2. ($q = 2, 4$) SYK model is always in a chaotic phase and the system always thermalizes exponentially fast. We also calculate the Lyapunov exponent of this system with high precision.
3. In quantum quenches starting from the chaotic state, the effective temperature is non-monotonic.
4. The spectral asymmetry frequency (SAF) does not change during quantum quenches using time-dependent SYK interactions.

We set out to show that a system in the integrable state fails to thermalize but instead we find that the system thermalizes instantaneously, most probably, due to an underlying physics different from chaotic dynamics. Failure of thermalization in highly interacting systems is a topic of intense research interest in experimental as well as theoretical physics. There are two popular paradigms in which a chaotic system fails to thermalize. The first one is the existence of quantum scars [25–31]. Quantum scars are eigenstates which violates eigenstate thermalization hypothesis (ETH). They also have finite energy density but anomalously low entanglement [32]. So states (pure or mixed) formed out of quantum scars do not thermalize. The other paradigm is many body localization (MBL) [33–36]. MBL is the suppression of chaos and slowing down of thermalization of an otherwise chaotic system due to the introduction of random disorder.

We would like to point out the difference of our work from [10] which considers a modified system consisting of SYK model coupled to quadratic peripheral fermions. This modified system also has a highly chaotic phase and a weakly interacting phase.

³Note that there is no phase transition which is otherwise claimed in this paper. Other deformation of SYK model has also been shown to have no phase transition [23].

Interestingly the above paper considers the modified model without any mass or chemical potential. In this setting, the system is either in the chaotic phase or in the weakly interacting phase depending on a parameter p which is the ratio of the number of the quadratic peripheral fermions and the number of SYK fermions. So depending on the value of p , the Hamiltonian of the modified system dictates if the system is in the chaotic phase or in the weakly-interacting phase. This is different from our present case where for the same Hamiltonian (at a given temperature and a given chemical potential) the system can be either in the chaotic state or the integrable state. Another importance difference is that in the above paper the modified system in the weakly-interacting phase thermalizes slowly but in our present work we observe that a system in the integrable state thermalizes instantaneously.

It would be interesting to examine closely the nature of the integrable state. We believe that an analytical treatment might be possible especially for this state which could reveal why systems in this state thermalize instantaneously. The dynamics of weakly interacting classical systems are well understood. The most famous example being the Fermi–Pasta–Ulam problem where the system fails to thermalize for exponentially long times even when there is a small but finite non-linear term. Similar phenomenon in weakly interacting quantum systems called prethermalization has been a topic of great interest in recent times [37–39].

We will be using lesser Green’s function $G^<(t_1, t_2)$, greater Green’s function $G^>(t_1, t_2)$, retarded Green’s function $G^R(t_1, t_2)$ and advanced Green’s function $G^A(t_1, t_2)$. The definition of these different Green’s functions are as follows

$$G^<(t_1, t_2) = i\langle\psi^\dagger(t_2)\psi(t_1)\rangle \tag{1.4}$$

$$G^>(t_1, t_2) = -i\langle\psi(t_1)\psi^\dagger(t_2)\rangle \tag{1.5}$$

$$G^R(t_1, t_2) = \Theta(t_1 - t_2) [G^>(t_1, t_2) - G^<(t_1, t_2)] \tag{1.6}$$

$$G^A(t_1, t_2) = \Theta(t_2 - t_1) [G^<(t_1, t_2) - G^>(t_1, t_2)] \tag{1.7}$$

The outline of this paper is as follows: We will work out the details of SYK model with complex fermions in section 2. The Kadanoff-Baym equations are derived in 2.1. We also explain the numerical methods involved in solving the equations. In section 3, we explain the phase transition and the details of the two phases. We examine in details the non-equilibrium dynamics of the chaotic state in section 3.1. We show that a system in the integrable phase thermalizes instantaneously in section 3.2. In section 4, we examine the non-equilibrium dynamics of ($q = 2, 4$) SYK model. Section 5 consists of conclusions from this work.

2 SYK model with complex fermions

The Hamiltonian is given in (1.2). To make the derivation simpler we will consider only ($q = 4$) interaction. We will consider the interaction with explicit time dependence. The action on the Schwinger-Keldysh contour \mathcal{C} is

$$S = \int_{\mathcal{C}} dt \left[\sum_{i=1}^N \psi_i^\dagger (i\partial_t - \mu) \psi_i - \sum_{i,j,k,l=1}^N j_{4,ij;kl}(t) \psi_i^\dagger \psi_j^\dagger \psi_k \psi_l \right] \quad (2.1)$$

$j_{4,ij;kl}(t) = j_{4R,ij;kl}(t) + ij_{4I,ij;kl}(t)$ are complex numbers. $j_{4R,ij;kl}(t)$ and $j_{4I,ij;kl}(t)$ are drawn from Gaussian distributions of zero mean and variances $J_4(t)$. Moreover,

$$j_{4,ij;kl} = j_{4,kl,ij}^*, \quad j_{4,ij;kl} = -j_{4,ji,kl}, \quad j_{4,ij;kl} = -j_{4,ij,lk} \quad (2.2)$$

We work with quenched averaging of the coupling in the large N limit [8, 9]. The contour ordered Green's function is defined as

$$G(t, t') = -\frac{i}{N} \sum_{i=1}^N \mathcal{T}_{\mathcal{C}} \left(\psi_i(t) \psi_i^\dagger(t') \right) \quad (2.3)$$

The partition function becomes

$$Z = \int \mathcal{D}\psi^\dagger \mathcal{D}\psi \int \mathcal{D}G \mathcal{D}\Sigma \exp \left[- \int_{\mathcal{C}} dt \sum_i \psi_i^\dagger (\partial_t - i\mu) \psi_i - \frac{N}{4} \int_{\mathcal{C}} dt_1 dt_2 J_4(t_1) J_4(t_2) G(t_2, t_1)^2 G(t_1, t_2)^2 - i \int_{\mathcal{C}} dt_1 dt_2 \Sigma(t_1, t_2) \left\{ G(t_2, t_1) + \frac{i}{N} \sum_i \psi_i(t_2) \psi_i^\dagger(t_1) \right\} \right] \quad (2.4)$$

Integrating out the fermions, the action in terms of the bilocal fields is

$$S[G, \Sigma] = -iN \operatorname{tr} \log [\partial_{t_1} \delta_{\mathcal{C}}(t_1, t_2) - i\mu \delta_{\mathcal{C}}(t_1, t_2) + i\Sigma(t_1, t_2)] + \frac{iN}{4} \int_{\mathcal{C}} dt_1 dt_2 J_4(t_1) J_4(t_2) G(t_2, t_1)^2 G(t_1, t_2)^2 - iN \int_{\mathcal{C}} dt_1 dt_2 \Sigma(t_1, t_2) G(t_2, t_1) \quad (2.5)$$

The equations of motion of G and Σ are

$$(i\partial_{t_1} + \mu) \delta_{\mathcal{C}}(t_1, t_2) - G(t_1, t_2)^{-1} = \Sigma(t_1, t_2) \quad (2.6)$$

$$\Sigma(t_1, t_2) = J_4(t_1) J_4(t_2) G(t_2, t_1) G(t_1, t_2)^2 \quad (2.7)$$

These are the Schwinger–Dyson (SD) equations in the Schwinger-Keldysh contour. Generalizing these equations for systems with ($q = 2, 4, 6$) interactions, the SD equations are

$$(i\partial_{t_1} + \mu) \delta_{\mathcal{C}}(t_1, t_2) - G(t_1, t_2)^{-1} = \Sigma(t_1, t_2) \quad (2.8)$$

$$\begin{aligned} \Sigma(t_1, t_2) = & J_2(t_1)J_2(t_2)G(t_1, t_2) + J_4(t_1)J_4(t_2)G(t_2, t_1)G(t_1, t_2)^2 \\ & + J_6(t_1)J_6(t_2)G(t_2, t_1)^2G(t_1, t_2)^3 \end{aligned} \quad (2.9)$$

We obtain different Green’s functions when we go from the Schwinger-Keldysh contour to the real time axis

$$G^>(t_1, t_2) = G(t_1^-, t_2^+), \quad G^<(t_1, t_2) = G(t_1^+, t_2^-) \quad (2.10)$$

where $t^\pm = t \pm i\epsilon$. Operator at t^+ comes before operator at t^- . With this, the SD equations are

$$\frac{1}{i\omega - \mu - \Sigma_R(\omega)} = G_R(\omega) \quad (2.11)$$

$$\begin{aligned} \Sigma^{>(<)}(t_1, t_2) = & J_2(t_1)J_2(t_2)G^{>(<)}(t_1, t_2) + J_4(t_1)J_4(t_2)G^{<(>)}(t_2, t_1)G^{>(<)}(t_1, t_2)^2 \\ & + J_6(t_1)J_6(t_2)G^{<(>)}(t_2, t_1)^2G^{>(<)}(t_1, t_2)^3 \end{aligned} \quad (2.12)$$

where G_R is defined in (1.6) and Σ_R is also similarly defined. The equilibrium solution are solved numerically. The connection between the above two equations are the fluctuation-dissipation relations which gives the expression of $G^>(\omega)$ and $G^<(\omega)$ in terms of the spectral function $A(\omega)$.

$$G^>(\omega) = -i \frac{A(\omega)}{1 + e^{\beta(\omega+\eta)}}, \quad G^<(\omega) = i \frac{A(\omega)}{1 + e^{-\beta(\omega+\eta)}} \quad (2.13)$$

$$A(\omega) = -2 \text{Im} G_R(\omega) \quad (2.14)$$

In the absence of μ and η , the SD equations are same as that of Majorana SYK models [8, 9]. This is because in thermal equilibrium,

$$G^>(t_1, t_2) = -G^<(t_2, t_1) \quad (2.15)$$

This relation holds true even out-of-equilibrium during time evolution starting from thermal equilibrium. So in the absence of mass or chemical potential, quantum quenches using time-dependent J_2, J_4 or J_6 in SYK model with complex fermions are same as quenches with the same time-dependent couplings in SYK model with Majorana fermions. Also note that in thermal equilibrium,

$$G^{>(<)}(t_1, t_2) = -G^{>(<)}(t_2, t_1)^* \quad (2.16)$$

Again this relation also holds true out-of-equilibrium starting from thermal equilibrium. This relation halves the computer time for time evolution because we can solve $G^{>(<)}(t_1, t_2)$ for either only $t_1 \geq t_2$ or $t_1 \leq t_2$.

We also verify conservation of energy during the quench processes. The expression for energy is

$$\begin{aligned}
\frac{E(t_1)}{N} &= -i \int_c dt_2 \left[\frac{J_2(t_1)J_2(t_2)}{2} G(t_2, t_1)G(t_1, t_2) \right. \\
&\quad \left. + \frac{J_4(t_1)J_4(t_2)}{4} G(t_2, t_1)^2 G(t_1, t_2)^2 + \frac{J_6(t_1)J_6(t_2)}{6} G(t_2, t_1)^3 G(t_1, t_2)^3 \right] \\
&= -i \int_{-\infty}^{t_1} dt_2 \left[\frac{J_2(t_1)J_2(t_2)}{2} (G^<(t_2, t_1)G^>(t_1, t_2) - G^>(t_2, t_1)G^<(t_1, t_2)) \right. \\
&\quad \left. + \frac{J_4(t_1)J_4(t_2)}{4} (G^<(t_2, t_1)^2 G^>(t_1, t_2)^2 - G^>(t_2, t_1)^2 G^<(t_1, t_2)^2) \right. \\
&\quad \left. + \frac{J_6(t_1)J_6(t_2)}{6} (G^<(t_2, t_1)^3 G^>(t_1, t_2)^3 - G^>(t_2, t_1)^3 G^<(t_1, t_2)^3) \right]
\end{aligned} \tag{2.17}$$

Using (2.15), one can also calculate the energy for SYK model with Majorana fermions.

The temperature and chemical potential can be calculated from $G^>(t_1, t_2)$ and $G^<(t_1, t_2)$ using the relation

$$\frac{G^K(\omega)}{-2 \text{Im}G^R(\omega)} = \tanh\left(\frac{\beta(\omega + \eta)}{2}\right) \tag{2.18}$$

The effective temperature during the non-equilibrium time evolution is calculated by using the method in [8, 9]. For this, we perform a coordinate transformation from (t_1, t_2) to $t_+ = t_1 + t_2, t_- = t_1 - t_2$. Fourier transform w.r.t. t_- and using 2.18 at small ω region gives the effective temperature as a function of t_+ . Note that t_+ increases or decreases in time step of $2 \times dt$. Highly chaotic system without quasiparticles are expected to thermalize exponentially as a function of the final temperature where the thermalization rate is directly proportional to the final temperature. This indeed has been shown to be true for SYK model without chemical potential.

$$T_{eff}(t_+) = T_f + \alpha e^{-\Gamma t_+}, \quad \Gamma = cT_f \tag{2.19}$$

2.1 Kadanoff-Baym equations and quantum quenches

We perform the quenches by solving the equations of motion of the Green's functions in integral form which are well-known as Kadanoff-Baym (KB) equations. The details

of the derivation of the KB equations from the SD equations can be found in [9]. After performing a convolution in eqn (2.8) with G we get

$$i\partial_{t_1}G(t_1, t_2) = \mu G(t_1, t_2) + \int_{\mathcal{C}} dt_3 \Sigma(t_1, t_3)G(t_3, t_2) \quad (2.20)$$

$$-i\partial_{t_2}G(t_1, t_2) = \mu G(t_1, t_2) + \int_{\mathcal{C}} dt_3 G(t_1, t_3)\Sigma(t_3, t_2) \quad (2.21)$$

The real time KB equations are obtained after contour deformation (Langreth rule). The imaginary leg in the contour is removed using Bogoliubov principle with weakening initial correlations.

$$i\partial_{t_1}G^>(t_1, t_2) = \mu G^>(t_1, t_2) + \int_{-\infty}^{\infty} dt_3 [\Sigma^>(t_1, t_3)G^A(t_3, t_2) + \Sigma^R(t_1, t_3)G^>(t_3, t_2)] \quad (2.22)$$

$$-i\partial_{t_2}G^>(t_1, t_2) = \mu G^>(t_1, t_2) + \int_{-\infty}^{\infty} dt_3 [G^>(t_1, t_3)\Sigma^A(t_3, t_2) + G^R(t_1, t_3)\Sigma^>(t_3, t_2)] \quad (2.23)$$

$$i\partial_{t_1}G^<(t_1, t_2) = \mu G^<(t_1, t_2) + \int_{-\infty}^{\infty} dt_3 [\Sigma^R(t_1, t_3)G^<(t_3, t_2) + \Sigma^<(t_1, t_3)G^A(t_3, t_2)] \quad (2.24)$$

$$-i\partial_{t_2}G^<(t_1, t_2) = \mu G^<(t_1, t_2) + \int_{-\infty}^{\infty} dt_3 [G^R(t_1, t_3)\Sigma^<(t_3, t_2) + G^<(t_1, t_3)\Sigma^A(t_3, t_2)] \quad (2.25)$$

Pure ($q = 2$) SYK model does not thermalize [9]. We can see from the above equations that ($q = 2$) SYK model even in the presence of chemical potential or a mass term does not thermalize at all. The system freezes completely as soon as the time-dependent perturbation stopped. This is because the expressions on the right side of (2.22) and (2.23) (or (2.24) and (2.25)) are same. So,

$$G^{>(<)}(t_1, t_2) = G^{>(<)}(t_1 + dt, t_2 + dt) \quad (2.26)$$

Unlike the ($q = 2$) SYK model, quantum quenches in the presence of ($q = 4$) interaction are non-trivial. Using relation (2.16), we will only use (2.23) to evolve $G^>(t_1, t_2)$ and (2.25) for $G^<(t_1, t_2)$. The most convenient forms of the equations for numerical

applications are ($t_a > t_b$)

$$\begin{aligned}
-i\partial_{t_a} G^>(t_b, t_a) &= \mu G^>(t_b, t_a) + \int_{t_b}^{t_a} dt_3 G^>(t_b, t_3) [\Sigma^<(t_3, t_a) - \Sigma^>(t_3, t_a)] \\
&\quad + \int_{-\infty}^{t_b} dt_3 [G^>(t_b, t_3)\Sigma^<(t_3, t_a) - G^<(t_b, t_3)\Sigma^>(t_3, t_a)] \quad (2.27)
\end{aligned}$$

$$\begin{aligned}
-i\partial_{t_a} G^<(t_b, t_a) &= -\mu G^<(t_b, t_a) + \int_{t_b}^{t_a} dt_3 G^<(t_b, t_3) [\Sigma^<(t_3, t_a) - \Sigma^>(t_3, t_a)] \\
&\quad + \int_{-\infty}^{t_b} dt_3 [G^>(t_b, t_3)\Sigma^<(t_3, t_a) - G^<(t_b, t_3)\Sigma^>(t_3, t_a)] \quad (2.28)
\end{aligned}$$

Note that the second integrals are same in the two equations. These equations can be solved incrementally/causally using a Predictor-Corrector scheme. We use forward difference for the prediction and we use backward difference for the correction. In the presence of non-zero μ , the forward difference and the backward difference must be strictly taken otherwise the numerical scheme fails to converge. The predicted value is

$$G^>(t_b, t_a + dt) = G^>(t_b, t_a)(1 + i\mu dt) + idt I_p(t_b, t_a) \quad (2.29)$$

where $I_p(t_b, t_a)$ consists of the sum of the two integrals in (2.27). The correction is performed using the backward difference formula and also using half substitution.

$$G^>(t_b, t_a + dt) = \frac{G^>(t_b, t_a)(1 + i\mu dt) + idt I_p(t_b, t_a)}{2} + \frac{G^>(t_b, t_a) + idt I_c(t_b, t_a + dt)}{2(1 - i\mu dt)} \quad (2.30)$$

where $I_c(t_b, t_a + dt)$ is the sum of the integrals in (2.27) calculated using the predicted value of $G^>(t_b, t_a + dt)$. Similarly, $G^<(t_b, t_a + dt)$ is also calculated. For the diagonal term $G^{>(<)}(t_a, t_a)$, we use the sum of (2.22) and (2.23).

$$G^>(t_a + dt, t_a + dt) = G^>(t_a, t_a) + idt I_{diag}(t_a) \quad (2.31)$$

$$G^<(t_a + dt, t_a + dt) = G^<(t_a, t_a) + idt I_{diag}(t_a) \quad (2.32)$$

$$\begin{aligned}
I_{diag}(t_a) &= \int_{-\infty}^{t_a} dt_3 [+G^>(t_a, t_3)\Sigma^<(t_3, t_a) - G^<(t_a, t_3)\Sigma^>(t_3, t_a) \\
&\quad - \Sigma^>(t_a, t_3)G^<(t_3, t_a) + \Sigma^<(t_a, t_3)G^>(t_3, t_a)] \quad (2.33)
\end{aligned}$$

An important check for our numerical codes is to perform equilibrium time evolution without quantum quenches. It serves three purposes. First it verifies that our codes are correct. It also verifies that our initial data are correct and accurate. The initial data are generated by solving the SD equations. Lastly, it verifies that numerical errors are under control.

3 Charged SYK model

In this section we will consider the system which has non-zero chemical potential or mass term in the Hamiltonian. We will consider only ($q = 4$) interaction. As we have mentioned in section 1, the system can undergo a phase transition in the presence of effective chemical potential (explicit chemical potential η or mass μ or both). In the chaotic phase, the system does not have a quasiparticle picture. In the integrable phase, the system consists of weakly interacting particles. Figure 2 are plots of spectral functions in the two different phases. The spectral function in the integrable phase has a sharp single peak.

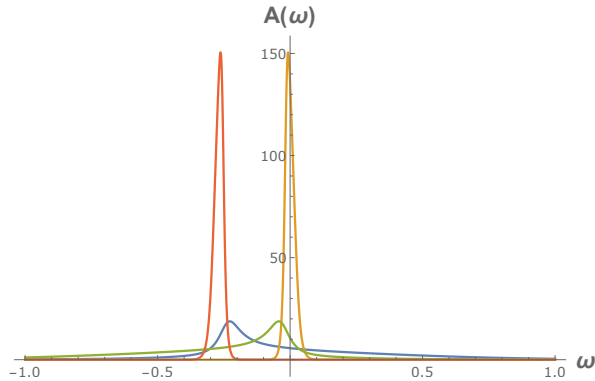


Figure 2: Plots of spectral function $A(\omega)$ in the two phases with chemical potential and with mass term. The blue curve is for the chaotic state with chemical potential $\eta = 0.27$. The yellow curve is for the integrable state with $\eta = 0.27$. The green curve is for the chaotic phase with mass $\mu = -0.27$. The red curve is for the integrable phase with $\mu = -0.27$.

The two phases are separated by a large energy gap. Due to this large energy gap quantum quenches cannot take the system from say the integrable state to the chaotic state. Figure 3 are plots of energy in the different phases with the mass term or the chemical potential.

The integrable phase also has occupation number close to 0 or 1 depending on the sign of the effective chemical potential. It can be easily seen from the plot of the spectral function. The area under the plot is equal to 1, this is fixed by fermionic commutation relation. The occupation number is given by

$$\frac{1}{N} \sum_i \langle \Psi_i^\dagger \Psi_i \rangle = \int d\omega \frac{A(\omega)}{1 + e^{\beta(\omega + \mu + \eta)}} \quad (3.1)$$

In case of chaotic state, the spectral function is spreaded and the fermionic distribution function more effectively suppresses the occupation number.

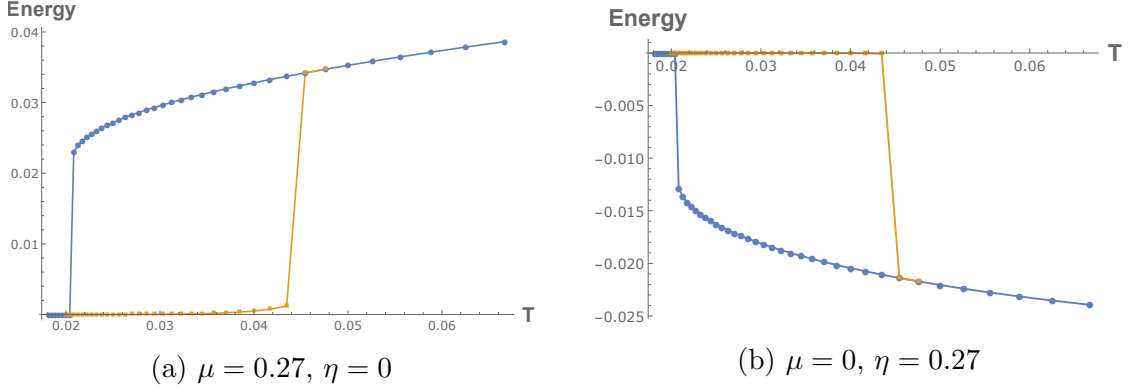


Figure 3: Plots of energy as a function of temperature T for the two different phases. The blue curves are for the chaotic phase. The orange curves are for the integrable phase.

The Lyapunov exponent in the chaotic state is large. The normalized Lyapunov exponent increases as we decrease the temperature for a fixed effective chemical potential. At the transition point from chaotic phase to the integrable phase, the Lyapunov exponent decreases sharply. But note that the Lyapunov exponent in the integrable phase is non-zero and it is large at higher temperature. Figure 1 is the plot of the normalized Lyapunov exponent for the two different phases with varying temperature and a fixed chemical potential.

3.1 Thermalization in the chaotic state

In this subsection we will consider quantum quenches in ($q = 4$) SYK model in the chaotic phase. We will study time evolution of the system after time-dependent perturbations with ($q = 2$) and ($q = 6$) interaction terms. So we will consider only bump quenches where the time-dependent term is turned on for a short time duration and completely turned off again. The system evolves non-trivially even after the perturbation has been turned off. The system thermalizes exponentially fast.

The initial equilibrium state is prepared by solving the SD equations (2.11) and (2.12). To perform the quantum quench, the KB equations (2.27) and (2.28) are solved numerically. The time dependent perturbations are turned on from $t_1, t_2 = 1 \times dt$ to $t_1, t_2 = s \times dt$ where dt is the size of the discrete time interval.

Figure 4 is the plot of effective temperatures for quenches in different settings but with the final temperature $T_f \sim 0.55$. As we can see the effective temperature is non-monotonic in all the cases. Without chemical potential, the effective temperature settles down to the final value. But with chemical potential, the effective temperature oscillates before settling down to the final value. As we have mentioned earlier, we use (2.18) at small ω region to calculate the temperature. The oscillation of the effective

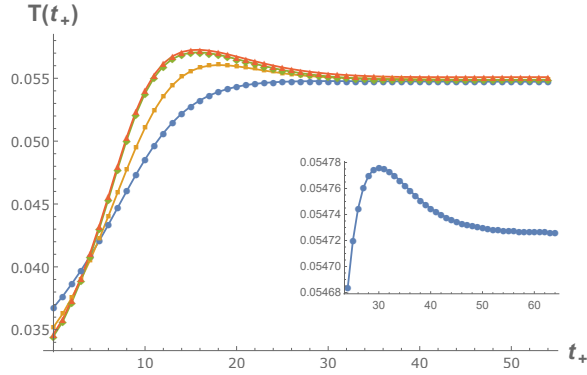


Figure 4: Plots of the effective temperature as a function of t_+ starting from different states and for different μ . The quenches have been tuned so that the final inverse temperature is $\beta \sim 18$. All the quenches are performed with time dependent ($q = 4$) interaction except for the red curve which was with time dependent ($q = 6$) interaction. The blue curve is for $\mu = \eta = 0$. The inset shows the non-monotonicity of the effective temperature for this case. The orange curve is for initial state with $\eta = 0.24$. The green curve is for initial state $\eta = 0$ but with $\mu = -0.263$. The red curve is for the same initial state as the green curve but the time dependent perturbation was ($q = 6$) interaction.

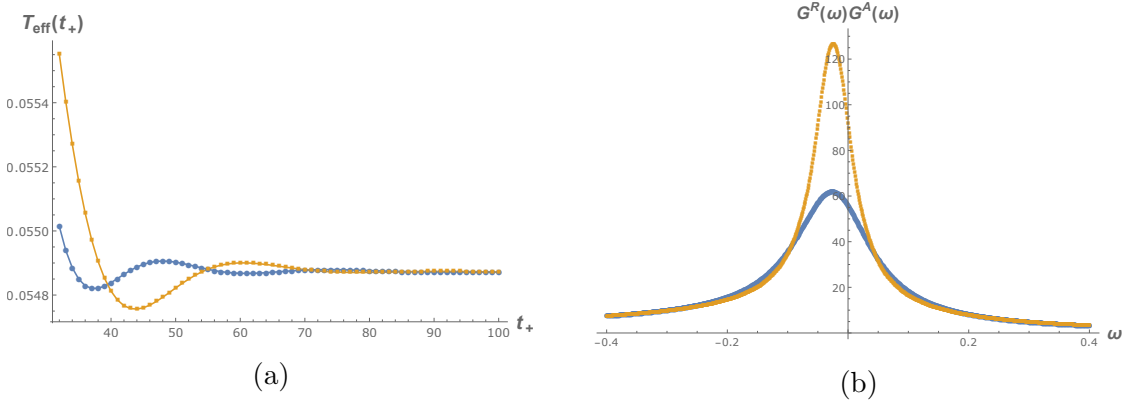


Figure 5: (a) The effective temperature as a function of t_+ calculated using different frequency cutoffs. This is for the quench for $\mu = -0.263$ starting from $\beta_i = 40, \eta = 0$. The final state is $\beta_f = 18.24, \eta = -0.029$. Note that the chemical potential changes during quench. (b) Considering the same quench, the spectral asymmetry frequency ω_s does not change during quantum quenches with SYK interactions. In this case, $\omega_s = -0.025$. The blue dots are $G^R(\omega)G^A(\omega)$ before quench and the orange dots are $G^R(\omega)G^A(\omega)$ after quench.

temperature actually depends on the frequency cutoff that we used for calculating the temperature. Figure 5a are the plots of effective temperature calculated using different

momentum cutoffs.

Note that the value of the chemical potential changes during quenches. A quantity which does not change during quantum quenches using time-dependent SYK interactions is the spectral asymmetry frequency (SAF). As defined in (1.3), SAF is the position of the maximum of $G^R(\omega)G^A(\omega)$. Figure 5b are the plots showing the position of SAF before and after a quantum quench.

3.2 Thermalization in the integrable state

We will now consider quantum quenches where the initial state is an integrable state. With $\mu \neq 0$, the Green's functions oscillate since the effective theory is a weakly interacting massive theory. So, we have to consider very small time-step size dt which results in very large number of discretization points. In case of $\mu = 0$ and $\eta \neq 0$, one can take large dt but since the effective theory for the integrable state is a weakly interacting massless theory, the Green's function do not decay fast so one has to consider again a very large number of discretization points although dt can be large.

Another technical difficulty while dealing with the integrable state is that the temperature cannot be calculated using (2.18) even for an equilibrium state solution calculated directly from the SD equations. The numerical precision is not good enough to cancel the spectral function and reproduce the tanh function. Consider the case of $\mu = 0$ and $\eta = 0.27$, as we can see in Figure 2 the spectral function is peaked around $\omega = 0$. From (2.18), the expression on the left hand side is zero and rapidly varies only around $\omega = -\eta$. But around this region of ω , $G^K(\omega)$, $G^R(\omega)$ and $A(\omega)$ are numerically very small. So during the quench process, we will compare the energy of the final state with the energy of integrable thermal states generated using the SD equations with different temperature and chemical potential. After finding a match in the energy, we compare $G^{>(<)}(t_1, t_2)$'s of the final state from the quantum quench and the thermal state.

As we have mentioned at the end of section 2.1, equilibrium time evolution without quantum quench is an important check. This check is very important for the integrable states due to the technical difficulties mentioned above.

We will present three cases:

1. For the integrable state with $\mu \neq 0$, we will consider $\mu = -0.27$, $\eta = 0$ and $\beta = 30$. We used time interval of $dt = 0.03$ and 20001 discretization time steps from $\{-10000 \times dt, 10000 \times dt\}$. For the quantum quench, we perturb the system with $J_2 = 1$ from time $t = 1 \times dt$ to $t = 9 \times dt$. The system thermalizes to the integrable state with $\eta = -0.049172$ and $\beta = 25.250$. The mass $\mu = -0.27$ is not changed during the quench.

2. For the integrable state with $\mu = 0, \eta \neq 0$, we will consider $\mu = 0, \eta = 0.27$ and $\beta = 50$ as the initial state. We used time interval $dt = 0.4$ and 20001 discretization time steps from $\{-10000 \times dt, 10000 \times dt\}$. For the quantum quench, we perturb the system with $J_2 = 0.1$ from time $t = 1 \times dt$ to $t = 9 \times dt$. The system thermalizes to the integrable state with $\eta = 0.351023$ and $\beta = 38.457$. The mass $\mu = 0$ is not changed during the quench.
3. We also considered a case in which the system is perturbed with time-dependent J_6 term. For this, we used the same initial as in the second case, i.e., $\mu = 0, \eta = 0.27$ and $\beta = 50$. For the quantum quench, we perturb the system with $J_6 = 100000$ from time $t = 1 \times dt$ to $t = 9 \times dt$. The system thermalizes to the integrable state with $\eta = 0.428934$ and $\beta = 31.471$. The mass $\mu = 0$ is not changed during the quench.

We find that the systems stop evolving instantaneously when the time-dependent perturbation is turned off. The Green's functions freeze as soon as the two time arguments t_1 and t_2 cross the quench region. Figure 6 are plots of the real parts of the greater Green's function $G^>(t - t_a, t)$ for different cases that we are considering. The imaginary part of $G^>(t - t_a, t)$ as well as the lesser Green's functions also freeze as soon as the two time arguments cross the quench region.

We could not calculate the effective temperature and the effective chemical potential of the final state.⁴ So, we search for thermal states with energy equal to that of the final state from the quantum quench. This is done by solving the SD equations for different values of temperature and chemical potential. In this two dimensional parameter space, we could find a line for which the energy matches the energy of the final state. Then we compare the Green's functions of these thermal states with the Green's functions of the final state. Again we could find a unique thermal state for which the Green's functions match those of the final state. So, in conclusion, the system in the integrable state thermalizes instantaneously. The instantaneous thermalization happens irrespective of the perturbing term. We used time-dependent J_2 or J_6 . Figure 7 are the plots of the real parts of the greater Green's functions $G^>(t - t_a, t)$ obtained after quantum quenches and thermal states generated using SD equations. It is evident that the final states are thermal states.

⁴It is not clear a priori if the final state is thermal or not. What we meant is that we could not calculate the left hand side of (2.18).

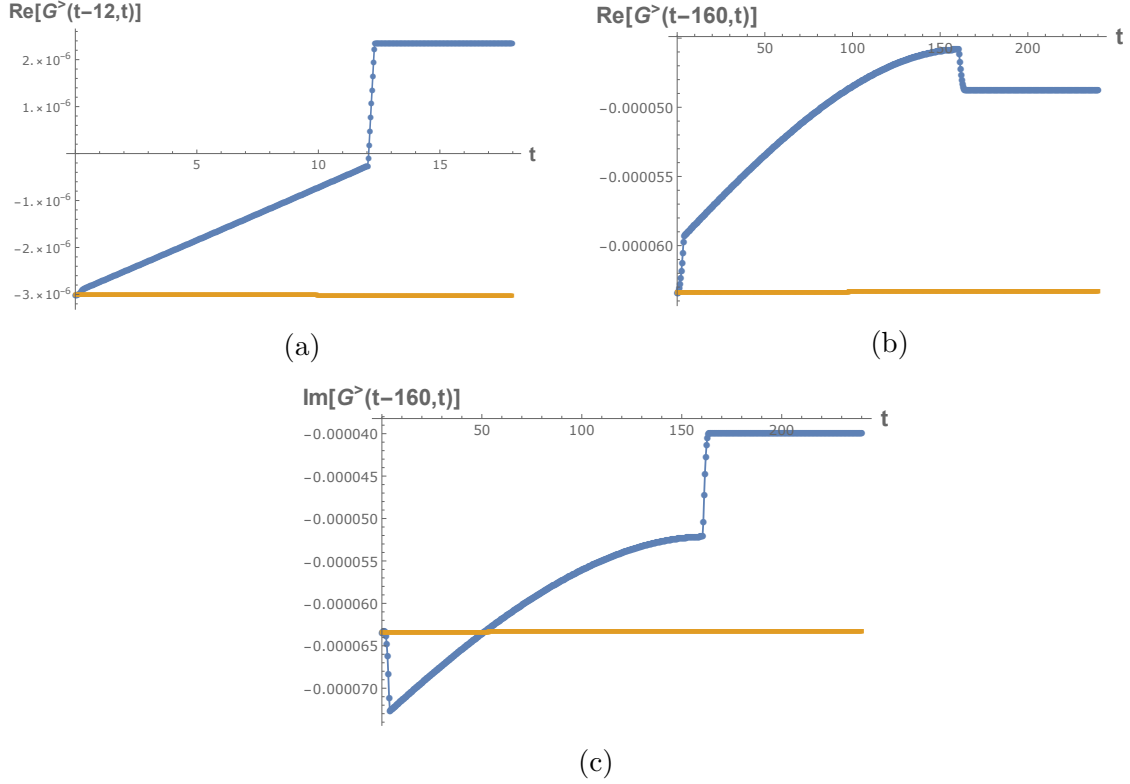


Figure 6: Time evolution of the real part of greater Green's function $G^>(t - t_a, t)$ as a function of t for fixed t_a showing the instantaneous thermalization (blue plots): (a) case 1 starting from the integrable state with $\mu = -0.27$, $\eta = 0$ and $\beta = 30$ and quantum quench using time dependent J_2 term, (b) case 2 starting from the integrable state with $\mu = 0$, $\eta = 0.27$ and $\beta = 30$ and quantum quench using time dependent J_2 term, and (c) case 3 starting from the integrable state with $\mu = 0$, $\eta = 0.27$ and $\beta = 30$ and quantum quench using time dependent J_6 term. The yellow plots are equilibrium time evolutions for the respective initial states without any time dependent perturbations.

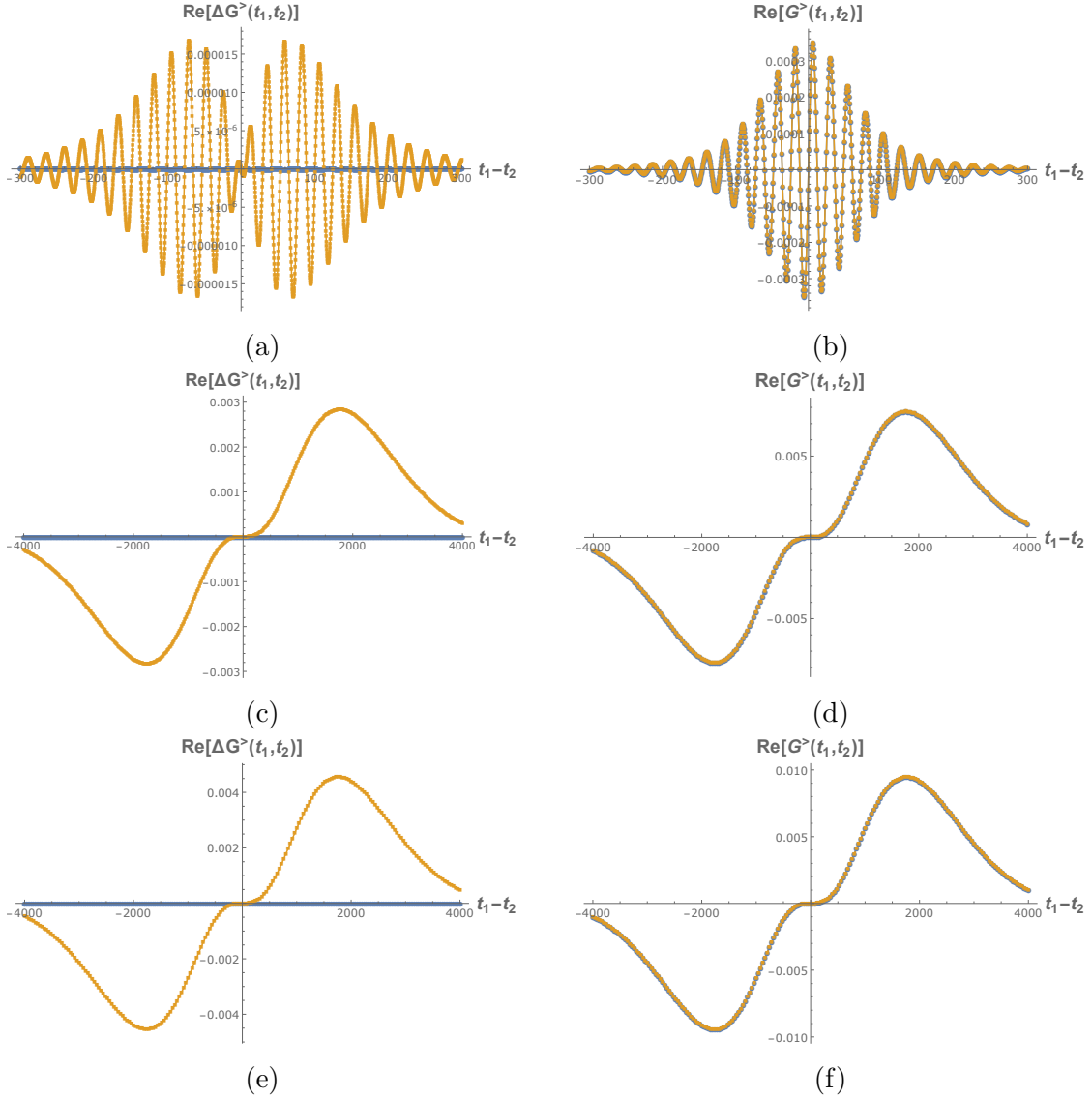


Figure 7: Plots on the left hand side: Blue curves are difference of the real part of the greater Green's functions of the final state and the thermal state with matching energy. Orange plots are difference of the real part of the greater Green's functions of the final state and the initial state. Plots on the right hand side: Blue curves are real part of the greater Green's functions of the final state. Orange plots are the real part of the greater Green's functions of the thermal state with matching energy. (a) and (b) are plots for case 1 starting from the integrable state with $\mu = -0.27$, $\eta = 0$ and $\beta = 30$ and quantum quench using time dependent J_2 term. (c) and (d) are plots for case 2 starting from the integrable state with $\mu = 0$, $\eta = 0.27$ and $\beta = 30$ and quantum quench using time dependent J_2 term. And (e) and (f) are plots for case 3 starting from the integrable state with $\mu = 0$, $\eta = 0.27$ and $\beta = 30$ and quantum quench using time dependent J_6 term.

4 $(q = 2, 4)$ SYK model

The $(q = 2, 4)$ SYK model is always in the chaotic state. The system does not undergo chaotic-integrable transition. But the $(q = 2)$ interaction suppresses chaos. This can be seen from 8. The Lyapunov exponent is greatly suppressed due to the presence of non-zero J_2 coupling but it does not sharply drop to a negligible value which is expected for a phase transition as in Figure 1. The suppression of chaos has also been shown from spectral correlation calculation in [22]. The introduction of large J_2 coupling forces the spectral statistics towards Poisson statistics. The spectral statistics obeys Poisson statistics for a generic integrable system while it obeys Wigner-Dyson(WD) statistics for a chaotic system. But this analysis are performed in finite systems (fixed N of the order of 10) so it is rather hard to precisely identify if the system is fully integrable or chaotic. In case of $(q = 2, 4)$ SYK model, the system is always in the chaotic state. This also implies that the system always thermalizes.

Figure 8 is the plot of Lyapunov exponent as a function of the inverse temperature for different values of J_2 . Note that in the absence of chemical potential, SYK model with N complex fermions is same as SYK model with $2N$ Majorana fermions in every respect at large N limit. We performed the calculations with Majorana fermions. It is interesting that with increasing inverse temperature the Lyapunov exponent decreases gradually after a peak while in the presence of chemical potential the Lyapunov exponent increases gradually in the chaotic state and sharply drops to a negligible value for the integrable state as shown in Figure 1.

To perform the quantum quenches, we consider two sets of the parameters which were considered in [7]. We consider $J_2 = 0.5, J_4 = 1$ and show thermalization below $\beta = 55$. Both the initial inverse temperature and the final inverse temperature are below $\beta = 55$. We also consider $J_2 = 2, J_4 = 1$ and show thermalization below $\beta = 15$.

Here also we will perform bump quenches. We work with $dt = 0.02$. With $J_2 = 0.5, J_4 = 1$, the initial state is at inverse temperature $\beta_i = 70$. We took the time range $t_1 - t_2 \in \{-5000 \times dt, 5000 \times dt\}$. The quantum quench is performed by turning on $J_6 = 0.4$ for the time duration $9 \times dt$ from time $t = 1 \times dt$ to $t = 9 \times dt$. The final inverse temperature is $\beta_f = 60.7$. Figure 9a is the plot of the effective temperature as a function of t_+ . With $J_2 = 2, J_4 = 1$, the initial state is at inverse temperature $\beta_i = 30$. The time range was $\{-3000 \times dt, 3000 \times dt\}$. The quantum quench is performed by turning on $J_6 = 0.7$ for the time duration $9 \times dt$ from time $t = 1 \times dt$ to $t = 9 \times dt$. The final inverse temperature is $\beta_f = 17.1$. Figure 9b is the plot of the effective temperature as a function of t_+ . The system thermalizes exponentially fast.

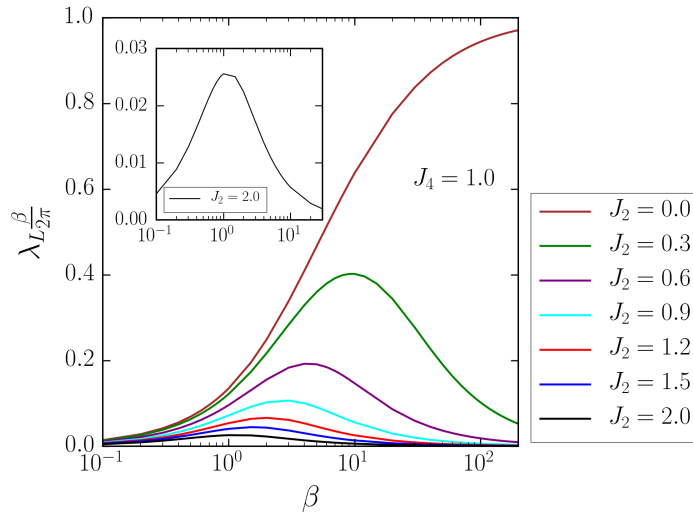


Figure 8: Plots of the normalized Lyapunov exponent as a function of inverse temperature β for different values of J_2 . For all the plots, $J_4 = 1$.

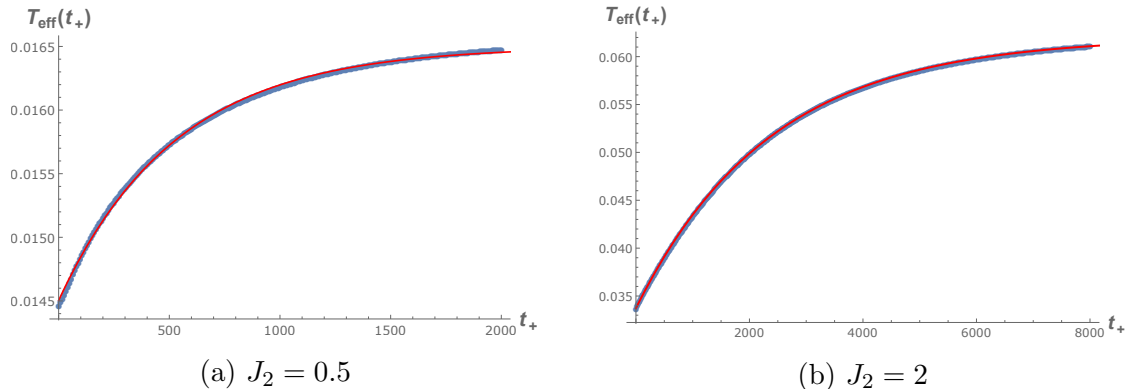


Figure 9: Thermalization of $(q = 2, 4)$ SYK model. (a) The blue dots are the calculated effective temperature for $J_2 = 0.5, J_4 = 1$ as a function of t_+ . The initial inverse temperature is $\beta_i = 70$. The final inverse temperature is $\beta_f = 60.7$. The red curve is an exponential fit with $0.0165 - 0.0020 \times e^{-0.0019t_+}$. (b) The blue dots are the calculated effective temperature for $J_2 = 2, J_4 = 1$ as a function of t_+ . The initial inverse temperature is $\beta_i = 30$. The final inverse temperature is $\beta_f = 17.1$. The red curve is an exponential fit with $0.0620 - 0.0283 \times e^{-0.00042t_+}$.

5 Conclusions

We show that the chaotic state in SYK model with complex fermions thermalizes. The presence of chemical potential suppresses the Lyapunov exponent. The effective temperature equilibrates exponentially fast. Closer examination reveals that the effective

temperature is non-monotonic. Without chemical potential, there is a single bump and the effective temperature settles down to its final value. In the presence of the chemical potential, there are damped oscillations during thermalization. The frequency of the oscillations depends on the frequency cut-off used to calculate the effective temperatures.

We also show that the integrable state in SYK model with complex fermions thermalizes instantaneously. This happens despite the fact that the system is weakly interacting in this phase. The process of instantaneous thermalization suggests that the underlying physics must be different from the well-known chaotic dynamics. We believe that this state could be handled analytically which could reveal this interesting dynamics. As we have mentioned in the Introduction, simple mass quenches in 0+1 dimensions can be said to thermalize instantaneously although the temperature does not change and only the effective chemical potential changes. Moreover, in case of pure ($q = 2$) SYK model, we have also shown that the system equilibrates instantaneously although the final state is not a thermal state.

On the other hand, the ($q = 2, 4$) SYK model always thermalizes exponentially fast. This happens even when the Lyapunov exponent is extremely small $\lambda_L^* \sim 0.003$ for $J_2 = 2, J_4 = 1$. With these interaction strengths, the spectral statistics of the model is almost completely Poisson statistics. So in conclusion, despite the nature of the spectral statistics, the system is always in a chaotic state.

Acknowledgement

The authors thank Krishnendu Sengupta, Ehud Altman, Sumilan Banerjee and Sayantani Bhattacharyya for communications on different topics related with this work. TS acknowledges financial support from the Department of Atomic Energy, Government of India, for the Regional Centre for Accelerator-based Particle Physics (RECAPP), Harish-Chandra Research Institute.

Bibliography

- [1] A. Polkovnikov, K. Sengupta, A. Silva, and M. Vengalattore, *Nonequilibrium dynamics of closed interacting quantum systems*, *Rev. Mod. Phys.* **83** (2011) 863, [[arXiv:1007.5331](#)].
- [2] C. Gogolin and J. Eisert, *Equilibration, thermalisation, and the emergence of statistical mechanics in closed quantum systems*, *Rept. Prog. Phys.* **79** (2016), no. 5 056001, [[arXiv:1503.07538](#)].

- [3] E. Altman, K. R. Brown, G. Carleo, L. D. Carr, E. Demler, C. Chin, B. DeMarco, S. E. Economou, M. A. Eriksson, K.-M. C. Fu, M. Greiner, K. R. A. Hazzard, R. G. Hulet, A. J. Kollar, B. L. Lev, M. D. Lukin, R. Ma, X. Mi, S. Misra, C. Monroe, K. Murch, Z. Nazario, K.-K. Ni, A. C. Potter, P. Roushan, M. Saffman, M. Schleier-Smith, I. Siddiqi, R. Simmonds, M. Singh, I. B. Spielman, K. Temme, D. S. Weiss, J. Vuckovic, V. Vuletic, J. Ye, and M. Zwierlein, *Quantum simulators: Architectures and opportunities*, 2019.
- [4] S. Sachdev and J. Ye, *Gapless spin-fluid ground state in a random quantum heisenberg magnet.*, *Phys. Rev. Lett.* **70** (1993) 3339.
- [5] A. Y. Kitaev, *Entanglement in strongly-correlated quantum matter*, . Talk at KITP, University of California, Santa Barbara.
- [6] J. Maldacena and D. Stanford, *Remarks on the Sachdev-Ye-Kitaev model*, *Phys. Rev.* **D94** (2016), no. 10 106002, [[arXiv:1604.07818](#)].
- [7] N. Sorokhaibam, *Phase transition and chaos in charged SYK model*, *JHEP* **07** (2020) 055, [[arXiv:1912.04326](#)].
- [8] A. Eberlein, V. Kasper, S. Sachdev, and J. Steinberg, *Quantum quench of the Sachdev-Ye-Kitaev Model*, *Phys. Rev.* **B96** (2017), no. 20 205123, [[arXiv:1706.07803](#)].
- [9] R. Bhattacharya, D. P. Jatkar, and N. Sorokhaibam, *Quantum Quenches and Thermalization in SYK models*, *JHEP* **07** (2019) 066, [[arXiv:1811.06006](#)].
- [10] A. Haldar, P. Haldar, S. Bera, I. Mandal, and S. Banerjee, *Quench, thermalization and residual entropy across a non-Fermi liquid to Fermi liquid transition*, [arXiv:1903.09652](#).
- [11] J. Maldacena and A. Milekhin, *SYK wormhole formation in real time*, [arXiv:1912.03276](#).
- [12] A. Almheiri, A. Milekhin, and B. Swingle, *Universal constraints on energy flow and syk thermalization*, 2019.
- [13] I. Kourkoulou and J. Maldacena, *Pure states in the SYK model and nearly-AdS₂ gravity*, [arXiv:1707.02325](#).
- [14] A. Dhar, A. Gaikwad, L. K. Joshi, G. Mandal, and S. R. Wadia, *Gravitational collapse in SYK models and Choptuik-like phenomenon*, *JHEP* **11** (2019) 067, [[arXiv:1812.03979](#)].
- [15] T. Numasawa, *Late Time Quantum Chaos of pure states in the SYK model*, [arXiv:1901.02025](#).
- [16] O. Bohigas, M. J. Giannoni, and C. Schmit, *Characterization of chaotic quantum spectra and universality of level fluctuation laws*, *Phys. Rev. Lett.* **52** (1984) 1–4.

- [17] J. Maldacena, S. H. Shenker, and D. Stanford, *A bound on chaos*, *JHEP* **08** (2016) 106, [[arXiv:1503.01409](#)].
- [18] S. Choudhury, A. Dey, I. Halder, L. Janagal, S. Minwalla, and R. Poojary, *Notes on melonic $O(N)^{q-1}$ tensor models*, *JHEP* **06** (2018) 094, [[arXiv:1707.09352](#)].
- [19] T. Azeyanagi, F. Ferrari, and F. I. Schaposnik Massolo, *Phase Diagram of Planar Matrix Quantum Mechanics, Tensor, and Sachdev-Ye-Kitaev Models*, *Phys. Rev. Lett.* **120** (2018), no. 6 061602, [[arXiv:1707.03431](#)].
- [20] R. Bhattacharya, S. Chakrabarti, D. P. Jatkar, and A. Kundu, *SYK Model, Chaos and Conserved Charge*, *JHEP* **11** (2017) 180, [[arXiv:1709.07613](#)].
- [21] S. Sachdev, *Bekenstein-Hawking Entropy and Strange Metals*, *Phys. Rev.* **X5** (2015), no. 4 041025, [[arXiv:1506.05111](#)].
- [22] A. M. García-García, B. Loureiro, A. Romero-Bermúdez, and M. Tezuka, *Chaotic-integrable transition in the sachdev-ye-kitaev model*, *Phys. Rev. Lett.* **120** (Jun, 2018) 241603.
- [23] T. Nosaka and T. Numasawa, *Quantum Chaos, Thermodynamics and Black Hole Microstates in the mass deformed SYK model*, [arXiv:1912.12302](#).
- [24] T. Akutagawa, K. Hashimoto, T. Sasaki, and R. Watanabe, *Out-of-time-order correlator in coupled harmonic oscillators*, *JHEP* **08** (2020) 013, [[arXiv:2004.04381](#)].
- [25] E. J. Heller, *Bound-state eigenfunctions of classically chaotic hamiltonian systems: Scars of periodic orbits*, *Phys. Rev. Lett.* **53** (Oct, 1984) 1515–1518.
- [26] H. Bernien, S. Schwartz, A. Keesling, H. Levine, A. Omran, H. Pichler, S. Choi, A. S. Zibrov, M. Endres, M. Greiner, and et al., *Probing many-body dynamics on a 51-atom quantum simulator*, *Nature* **551** (Nov, 2017) 579–584.
- [27] C. J. Turner, A. A. Michailidis, D. A. Abanin, M. Serbyn, and Z. Papić, *Weak ergodicity breaking from quantum many-body scars*, *Nature Physics* **14** (May, 2018) 745–749.
- [28] C. J. Turner, A. A. Michailidis, D. A. Abanin, M. Serbyn, and Z. Papić, *Quantum scarred eigenstates in a rydberg atom chain: Entanglement, breakdown of thermalization, and stability to perturbations*, *Phys. Rev. B* **98** (Oct, 2018) 155134.
- [29] W. W. Ho, S. Choi, H. Pichler, and M. D. Lukin, *Periodic orbits, entanglement, and quantum many-body scars in constrained models: Matrix product state approach*, *Physical Review Letters* **122** (Jan, 2019).
- [30] V. Khemani, C. R. Laumann, and A. Chandran, *Signatures of integrability in the dynamics of rydberg-blockaded chains*, *Physical Review B* **99** (Apr, 2019).

- [31] C.-J. Lin and O. I. Motrunich, *Exact quantum many-body scar states in the rydberg-blockaded atom chain*, *Physical Review Letters* **122** (Apr, 2019).
- [32] B. Mukherjee, S. Nandy, A. Sen, D. Sen, and K. Sengupta, *Collapse and revival of quantum many-body scars via floquet engineering*, 2019.
- [33] A. Pal and D. A. Huse, *Many-body localization phase transition*, *Physical Review B* **82** (Nov, 2010).
- [34] R. Nandkishore and D. A. Huse, *Many-body localization and thermalization in quantum statistical mechanics*, *Annual Review of Condensed Matter Physics* **6** (Mar, 2015) 15–38.
- [35] F. Alet and N. Laflorencie, *Many-body localization: An introduction and selected topics*, *Comptes Rendus Physique* **19** (Sep, 2018) 498–525.
- [36] D. A. Abanin, E. Altman, I. Bloch, and M. Serbyn, *Colloquium : Many-body localization, thermalization, and entanglement*, *Reviews of Modern Physics* **91** (May, 2019).
- [37] M. Marcuzzi, J. Marino, A. Gambassi, and A. Silva, *Prethermalization in a nonintegrable quantum spin chain after a quench*, *Physical Review Letters* **111** (Nov, 2013).
- [38] F. Essler, S. Kehrein, S. Manmana, and N. Robinson, *Quench Dynamics in a Model with Tuneable Integrability Breaking*, *Phys. Rev. B* **89** (2014), no. 16 165104, [[arXiv:1311.4557](https://arxiv.org/abs/1311.4557)].
- [39] O. Howell, P. Weinberg, D. Sels, A. Polkovnikov, and M. Bukov, *Asymptotic prethermalization in periodically driven classical spin chains*, *Physical Review Letters* **122** (Jan, 2019).